Exploring the interactions between starches, bentonites and plasticizers in sustainable barrier coatings for paper and board

BREEN, Christopher <http://orcid.org/0000-0002-5637-9182>, CLEGG, Francis <http://orcid.org/0000-0002-9566-5739>, THOMPSON, Simon, JARNSTROM, Lars and JOHANSSON, Caisa <http://orcid.org/0000-0001-7368-7227>

Published version

BREEN, Christopher, CLEGG, Francis, THOMPSON, Simon, JARNSTROM, Lars and JOHANSSON, Caisa (2019). Exploring the interactions between starches, bentonites and plasticizers in sustainable barrier coatings for paper and board. Applied Clay Science, 183, p. 105272.

Exploring the interactions between starches, bentonites and plasticizers in sustainable barrier coatings for paper and board.

Chris Breen[a,*], Francis Clegg[a], Simon Thompson[a,1], Lars Jarnstrom[b], Caisa Johansson[b,2]

[a]*Materials and Engineering Research Institute, Sheffield Hallam University, Sheffield, S1 1WB, UK*
[b]*Department of Engineering and Chemical Sciences, Karlstad University, SE-651 88 Karlstad, Sweden*

ABSTRACT

Effective food packaging is a major factor in the current global drive to minimise food waste. Starch is an excellent oxygen barrier for packaging but it is brittle and moisture sensitive. The addition of layered minerals and plasticizers can significantly improve the moisture barrier and flexibility of the resulting composite. Some combinations of starch and plasticizer are incompatible but our results show that the addition of bentonite ensures the formation of coherent starch films with much improved moisture barrier regardless of the starch-plasticizer compatibility. It was clearly demonstrated that improvement of the moisture barrier was critically dependent on the layer charge of the bentonite used. Starch was readily accommodated in the interlayer space of bentonites with a layer charge of < 0.4 electrons per formula unit but was not adsorbed if the layer charge was above this value. Starch-bentonite-plasticizer coatings prepared using bentonites with the lower layer charge routinely produced higher barriers to water vapour. The water vapour transmission rate (WVTR) of the base paper was reduced from 780 to 340 ± 20 g m^2 day^{-1} when coated with starch alone. This was further reduced to 48 or 66 g m^2 day^{-1} if glycerol or lower charge bentonite, respectively, was added to the starch. Optimised coatings of starch-lower charge bentonite-plasticizer provided WVTR values of ≤ 10 g m^2 day^{-1} whereas WVTR values for comparative coatings prepared using the higher charge bentonites were three to four times higher (35 ± 7 g m^2 day^{-1}). Scanning electron micrographs provided clear evidence for the presence of 60 nm thick supramolecular layers formed from starch-bentonite-plasticizer in the samples

coated on either glass or paper. The WVTR values for these low-eco footprint coatings are competitive with proprietary coatings prepared using petroleum derived resins.

Keywords: Barrier coating, bentonite, starch, layer charge, x-ray diffraction, SEM

Corresponding Author:
Dr. Francis Clegg, Materials and Engineering Research Institute, Sheffield Hallam University, Sheffield S1 1WB, UK. E-mail: f.clegg@shu.ac.uk

Contact details for other authors:
Professor Chris Breen, Materials and Engineering Research Institute, Sheffield Hallam University, Sheffield S1 1WB, UK. Phone +44-1142253008. E-mail: c.breen@shu.ac.uk
Dr. Simon Thompson, Materials and Engineering Research Institute, Sheffield Hallam University, Sheffield S1 1WB, UK E-mail: stnotts@gmail.com
Professor Lars Jarnstrom, Department of Engineering and Chemical Sciences, Karlstad University, SE-651 88 Karlstad, Sweden. E-mail: lars.jarnstrom@kau.se
Professor Caisa Johansson, Department of Engineering and Chemical Sciences, Karlstad University, SE-651 88 Karlstad, Sweden. E-mail: Caisa.Johansson@billerudkorsnas.com

[1]Dr. Simon Thompson, 26 Springfield Road, Hucknall, Nottingham, NG15 6PR, UK
[2]Professor Caisa Johansson, BillerudKorsnäs AB**,** Storjohanns väg 4 SE-664 28 Grums, Sweden

1. Introduction

Food waste in the US (Buzby and Hyman, 2012), the European Union (EU) (Muriana, 2015) and across the world (Kummu *et al*., 2012; Papargyropoulou *et al*., 2014) continues to confound producers, consumers and politicians because of the enormous amount of energy entrained during food production (Wikstrom *et al*., 2014). It is imperative that as little food as possible is wasted and does not contribute to the 90 million tons of food waste generated each year in the EU (European Commission, 2016) (http://ec.europa.eu/food/safety/food_waste/index_en.htm). Correctly engineered packaging can contribute to the reduction in food waste by prolonging the safe storage period of the more perishable foods (Johansson *et al*., 2012; Peelman *et al*., 2013, 2014; Verghese *et al*., 2015). However, the vast majority of the required packaging materials are manufactured in conventional chemical processes using petrochemical derived monomers and the public are increasingly aware of the sustainability and environmental issues associated with these materials. Consequently, efforts to replace these oil-derived materials with greener, biobased alternatives are becoming more widespread (Peelman *et al*., 2013, 2014; Rhim *et al*., 2013) particularly since biopolymers represent excellent barriers to the diffusion of oxygen. Unfortunately, this excellent barrier rapidly diminishes when moisture penetrates

into biopolymers, like the starch used here. The dramatic improvements in the ability of the starch to resist the ingress of moisture, reported here, will enable full advantage of its inherently low oxygen permeability to be exploited. Although the oxygen barrier is not a focus of this study, it is worth noting that an excess of oxygen can damage flavours and colours, turn fatty foods rancid, promote microbial growth on meat, and cause browning or bleaching of the packaged food.

It is now well established that the incorporation, delamination and dispersion of layered aluminosilicates in polymer matrices can markedly improve the barrier properties compared to those of the host polymer alone (Choudalakis and Gotsis, 2009; Peelman *et al*., 2013, 2014; Rhim *et al*., 2013;). The effort invested in the production of mechanically robust, self-supporting thermoplastic starch films via film-casting or hot pressing methods far outweighs that directed towards starch-bentonite-plasticizer composites as barrier coatings applied to paper or board. One early example of starch-bentonite barrier coatings at high clay loadings (91 %mass) was given by Hlavatsch *et al*., 1997), where the barrier formulation was used as pre-coating in order to improve print quality of the coated paper. In general, the starch-bentonite systems studied have encompassed a wide, poorly defended selection of unmodified and organomodified bentonites dispersed into a wide range of different starches. Different groups have focussed on starches from different sources (with an extensive range of amylose to amylopectin ratios), different plasticizers (including water and organic species such as glycerol, sorbitol, triacetin) and other additives including sugars (Souza *et al*., 2012), pequi oil (Schlemmer *et al*., 2010) urea and acetic acid (Lu *et al*., 2012), polyester (McGlashan and Halley, 2003), polycaprolactone (Kalambur and Rizvi, 2004) and polyvinyl alcohol, PVOH (Dean *et al*., 2008). The matrix is then further expanded by the rather eclectic selection of swelling (Wilhelm *et al*., 2003), non-swelling (de Carvalho *et al*., 2001; Lu *et al*., 2012; Mbey *et al*., 2012), acid-treated bentonite (Schlemmer *et al*., 2010), and sepiolite (Chivrac *et al*., 2010c) as well as bentonite organically modified using alkylammonium cations or polymeric species such as chitosan (Kampeerapappun *et al*., 2007) and

cationically modified starch (Chivrac *et al*., 2008, 2010a, 2010b). Recent additions to the list of layered materials utilised to enhance the properties of starch include layered double hydroxides (Chung and Lai, 2010), zirconium phosphates - both 'natural' and specifically modified for the purpose (Donnadio *et al*., 2012) and graphite oxide (Li *et al*., 2011). Extensive diversity also exists with regard to the ratio of the different components (starch, water, plasticizer, layered species) in the starting mixture which is then further complicated with the use of different processing equipment, mixing times and temperature profiles used to produce the thermoplastic starch prior to fabricating films using a variety of approaches.

Other relevant approaches include the work of Nam and co-workers (Nam *et al*., 2009) who have pioneered the use of self-supporting films of inorganic-cation exchanged stevensite alone to successfully produce barriers to oxygen. The relatively poor water vapour barrier of these 'polymer-free' systems led to subsequent developments where carboxymethlycellulose (CMC) or poly(acrylic acid) (Ebina and Mizukami, 2007) were incorporated to improve the coherent nature of their films leading to improvements in flexibility, transparency, thermal stability and mechanical strength thus extending the range of applications to include the fabrication of electric luminescence devices. Others have focussed on the reproducible synthesis of large diameter (20-40 µm) mica-like nanoplatelets in order to significantly enhance the 'polymer-free' approach (Moeller *et al*., 2010). Self-supporting montmorillonite films without polymers were reported by Isayama and Kunitake (1994).

Grunlan and co-workers have used the layer-by-layer, LbL, approach to fabricate chitosan-montmorillonite (Laufer *et al*., 2012) and polyethyleneimine PEI-montmorillonite (Priolo *et al*., 2011) nanobrick walls which, although the production times are lengthy, offer excellent barrier properties towards oxygen. Others (Findenig *et al*., 2012) deposited 40 cationic starch-montmorillonite bilayers on a cellulose substrate and thus reduced the water vapour transmission rate (WVTR) by 32% from 360 to 244 g m^{-2} day^{-1}.

Walther *et al.* (2010a,b) have recently demonstrated that paper coating, painting and the doctor blade approach, can readily produce macroscopic quantities of nacre like, high Cloisite®-Na^+ content polymer composites with mechanical properties that surpass those of LbL films and are directly competitive with those of nacre itself.

The samples described in this study, prepared using the same technique as Walther and co-workers (Walther *et al*., 2010a), offer a direct comparison with the work on montmorillonite-cationic starch presented by Findenig (Findenig *et al*., 2012) except that it uses uncharged starch thus making it an important comparator to the PVOH-montmorillonite films described by Walther *et al*. (2010a). The current contribution complements and extends results from the paper coating approach, previously described by some of us (Johansson *et al*., 2010; Olsson *et al*., 2014a,b), making significant focussed use of X-ray diffraction and scanning electron microscopy to identify those particular combinations of starch, plasticizer and bentonite which provide excellent, medium barrier properties.

Collation of the published data, summarised above, identified three key issues to be reconciled concerning these low eco-footprint barrier coatings and films. The first was whether there were any synergistic combinations of starch-bentonite-plasticizer which improved the barrier to moisture. The second was how the layer charge of the bentonite used influenced the barrier properties of the starch nanocomposites produced. The third was whether the preferential adsorption of plasticizer in the bentonite interlayer influenced the barrier properties of the resulting construct.

The relative speed of the paper coating approach, compared to the fabrication time associated with LbL films, enabled the investigation of an extended matrix of samples with which to address the three issues identified above. Consequently, this work reports on a carefully selected subset of four starches, four bentonites (each from a robust, commercial supply) and six plasticizers. It demonstrates that the production of an acceptable barrier to water vapour requires the ability of the lower charge bentonites to (simultaneously)

accommodate both starch and plasticizer in the interlayer space and that a particular starch-bentonite-plasticizer combination must be carefully optimised to maximise the barrier properties. The resulting sustainable, barrier material has a WVTR that is competitive with those obtained using formulations containing oil-derived polymers. Consequently, it represents a hybrid approach in that an optimised starch-bentonite-plasticizer formulation, with a relatively high bentonite content (ca 30 %mass in final film), is coated onto a low-base weight, flexible paper substrate which provides the required mechanical strength. Scanning electron micrographs provided clear evidence for the presence of 60 nm thick supramolecular layers formed from starch-bentonite-plasticizer in the samples coated on either glass or paper. These 'macro' layers require further consideration when attempting to model the diffusion through polymer-bentonite composites with high bentonite contents.

2. Experimental:

2.1 Materials

Four starches with different chemical modification (supplied by Cargill, Germany) were selected. All of these starches were thinned and showed good film forming properties with acceptable flexibility. These were EC, an ether-modified corn starch; HWC, a hydrophobically-modified waxy corn starch (98% amylopectin); EHAC, an ester-modified, high amylose corn starch and EP, an ether-modified potato starch. The amylose content of the starch grades was EC = 24%, HWC = 2%, EHAC = 50-80%, EP = 22%.

The crystallinity of a starch film contributes to the oxygen barrier but imparts significant brittleness, so the films are made more flexible by introducing commercially available, low molecular weight compounds, e.g. glycerol, sorbitol, triacetin, or oligomeric, e.g. poly(ethylene glycol), plasticizers; all of which are classified as GRAS (Generally Recognized As Safe) and potentially suitable for food contact applications. Polyethylene glycol (PEG), of different molecular weights; 600, 1000, and 2000 (designated PEG600,

PEG1000 and PEG2000), glycerol, sorbitol, and triacetin were obtained from Aldrich and used as received.

Four different bentonites, from reputable suppliers, were selected for investigation. They were chosen to encompass a realistic range of cation exchange capacity, viscosity and elemental composition. Two were sourced from Rockwood Additives; Cloisite® Na^+ (CEC = 92.5 meq/100g) and Nanofill® 116 (CEC = 100 meq/100g), these will subsequently be referred to as CNa and N116, respectively. The other two were obtained from Nanocor; PGN (CEC = 120 meq/100g) and PGV (CEC = 145 meq/100g). The exchangeable cation in all these bentonites was predominantly sodium. From XRF data (not shown) obtained from washed and also fully K-exchanged bentonites the percentage amounts of Ca relative to Na were determined to be 0%, 31%, 9% and 20%, for the bentonites CNa, N116, PGN and PGV, respectively. The aspect ratios of the bentonites layers, according to the suppliers, were 75-100 nm, 300-500 nm and 150-200 nm, for CNa, PGN and PGV, respectively. No data was available for N116. The X-ray diffraction (XRD) traces for the four different bentonites (Fig. S1) confirmed that the samples were almost completely free of crystalline impurities and displayed a 001 reflection near 7 °2θ (12.5 Å) confirming the presence of one layer of water in the interlayer space. All bentonites contained extraneous sodium-based salts, of which PGN and N116 contained the highest levels, and the FTIR spectra and diagnostic mass fragments (m/z) in the TG-MS data indicated the presence of carbonate (m/z = 44) and sulphate (m/z = 64) impurities (data not shown). The layer charges were qualitatively assessed using the X-ray pattern approach described previously (Christidis and Eberl, 2003) - the relative reflection positions, their breadth and absence or presence of 00/ reflections were used to establish that CNa and PGN carried a layer charge of < 0.4 electrons per formula unit ($Al_2Si_4O_{10}(OH)_2$) whereas the layer charge on the other two bentonites, N116 and PGV, was > 0.4 electrons per formula unit. All four bentonites were used as received except where explicitly stated.

The sized and coated paper substrate was Gerbier HDS, a 50 g m^{-2}, low base weight, flexible material. One side was coated with a mixture of calcium carbonate and kaolin in a carrier matrix to provide a surface compatible with printing procedures. The mineral components gave rise to crystalline reflections in the XRD trace of the paper (Fig. S2).

2.2 Standard coating formulation

The aqueous starch suspensions were prepared at 20 %mass. Each starch mixture was heated from room temperature to 95°C over 30 minutes and then maintained at 95°C for a further 30 minutes under vigorous stirring. The cooked starch was then cooled to 60°C and the plasticizer solution added and stirred for 60 minutes. The aqueous bentonite suspension, prepared by mixing with a saw toothed blade at 1000 rpm for 18 hours, was then added and the resulting starch-bentonite-plasticizer suspension stirred for a further 2 hours. Increasing the time for dispersion of the as-received bentonites and starch from 2 to 3, 4, 5 or 20 hours at 60°C did not increase the layer expansion for either pair of bentonites confirming that the adopted mixing time of 2 hours was sufficient. Indeed, the diffraction traces after 1 hour mixing were virtually identical to those after 20 hours mixing. A number of coating systems were subjected to additional ultrasound mixing (10 minutes) in order to remove bubbles entrained during the coating preparation. This established that ultrasound did not significantly enhance the bentonite dispersion (assessed by XRD); nor were the barrier properties (WVTR) of the dried coating improved.

The information within the text and Figures (including the supplementary data) reports the concentrations of starch, plasticizer and bentonite in units of parts per hundred (pph) to avoid the confusion associated with %mass units when comparing the composition of a particular multi-component coating. The number of pph of the component added is provided relative to the starch portion (100 pph). Therefore, a formulation containing 10 g starch plus 4 g bentonite and 3 g of plasticizer would be represented as 40 pph bentonite and 30 pph plasticizer. Consequently, the standard coating formulation contains 100 pph starch HWC,

48 pph of bentonite CNa and 20 pph of PEG600 plasticizer and, in this communication, would be identified as HWC-CNa-PEG600(20).

The concentrations of starch, bentonite and plasticizer used in the coatings are presented in Table 1. The plasticizer concentrations used, 10, 20 and 30 pph relative to the dry starch content, were identified during the preliminary survey and most formulations provided coherent and flexible films when mixed with starch alone. The bentonite concentration (48 pph) was kept constant relative to the starch concentration.

2.3 Paper coating procedure

The low base weight paper substrate (50 g m^{-2}) had been sized and coated with proprietary formulations optimised for printing purposes on one side. The coatings under investigation here were applied to the reverse (uncoated side) of the paper, which is standard procedure in the packaging industry. A bench coater (K Control Coater, RK Print Coat Instruments Ltd.) with bar No. 5, provided a wet film thickness of 50 µm. A wet coated sheet was then supported (freshly-coated side face up) on a cardboard sheet and immediately transferred to an oven and dried at 105°C for 40 seconds. The partially dried, coated paper (freshly-coated side face up) was then transferred onto a metal sheet in an oven at 60°C, held in place with weights at each of the four corners and left to dry for 4 minutes. All samples were touch-dry upon removal from the oven. Samples to which one and two coating layers had been applied were prepared. Depending upon the solids content of the coating system (15.2 - 21.8 %mass, Table 1) a single layer would be approximately 7.6 - 10 µm when dry. This does not account for any penetration of the coating into the pores between the cellulose fibres of the paper substrate, which may occur during the coating procedure. Aliquots of the suspensions described were also cast as thin layers on glass microscope slides and dried in an oven at 40ºC.

2.4 Water Vapour Transmission Rate (WVTR)

All samples were pre-conditioned in a Sharetree THC/Slimline/420/ME relative humidity oven at a constant climate of 23°C and 50% relative humidity (RH) for 24 hours before analysis. The gravimetric cup method with silica gel as desiccant was used and the WVTR data was collected under the same conditions of temperature and RH with the starch-bentonite-plasticizer coated side exposed to the humid air. All samples were analysed in triplicate and the average value is presented. Both one and two layer coated samples were prepared and, where appropriate, the WVTR values obtained for each layer are presented to emphasise the lack of pinholes in the first coated layer. The results of the preliminary survey of the effect of the coat weight on the WVTR values for HWC-CNa-PEG600(20) is presented in Fig. S3.

The extraneous salt identified in N116, which contained the highest level, was removed by washing six times and the cleaned N116 was used to prepare a 'standard' coating, based on starch HWC and 20 pph PEG600. The extensive washing did nothing to reduce the WVTR value for this sample. However, fully saturating N116 with Na^+-ions, using well established procedures (Breen *et al*., 1997), did reduce the WVTR from 87 to 45 g m^{-2} day^{-1} (Fig. S4). Unfortunately, the final value was twice that for HWC-CNa-PEG600(20) (18 g m^{-2} day^{-1}) and HWC-PGN-PEG600(20) (21 g m^{-2} day^{-1}). Consequently, the resource intensive washing procedure for N116 was discontinued.

2.5 X-Ray Diffraction (XRD)

XRD traces of bentonite powders or coatings prepared on paper or glass microscope slides were obtained on a Philips X'Pert Pro diffraction system equipped with a proportional detector (Miniprop) and Cu-tube (λ = 1.542 Å) operating at 40 kV and 40 mA. Other parameters included; divergent and anti-scatter slits of ½ and 1º, mask 15, step size 0.04, time per step 4s, and scan speed 0.01 °/s. The thermal stability of selected samples was studied by heating the glass slides in air at the required temperature (100 and 150°C) for 120 min.

2.6 Electron Microscopy

Scanning electron micrographs were obtained using a secondary electron detector from cross sections of samples coated on either glass slides (and then prised off the glass) or paper and then fractured in liquid nitrogen. The samples were gold coated prior to imaging in a FEI Nova 200 Nano SEM.

3. Results

In this section the barrier properties of the different formulations will be presented and attention drawn to the way in which incorporation of the low charge (CNa, PGN) bentonites results in a better barrier performance than that provided by the high charge (N116, PGV) bentonites. X-ray diffraction traces of representative coatings on glass slides and on a paper substrate are used to determine the way in which the starch and plasticizer expands the bentonite spacing and reveals that, in the absence of plasticizer, only the low charge bentonites are able to accommodate starch in the interlayer space and that the formulations prepared using the low charge bentonites appear to be more highly ordered and cover the paper fibres more effectively. Finally, scanning electron microscope images provide strong evidence for the formation of ca. 60 nm thick supramolecular layers, which perhaps arise from globules of starch-bentonite-plasticizer (*vide infra*). These globules may be formed as the coating is applied and subsequently dried.

3.1 Water Vapour Transmission Rates

The WVTR values for base paper were reduced by ca. 60% (780 to 340 ± 20 g m^{-2} day^{-1}) when two layers of the starches EC, HWC or EHAC were applied, whereas two layers of EP provided a lower WVTR of 256 g m^{-2} day^{-1} (Fig. 1a). The addition of 20 pph PEG600 to EC and HWC was particularly detrimental to the barrier properties of the coating (increasing the WVTR from 337 to 616 and from 321 to 673 g m^{-2} day^{-1}, respectively) whereas its effect on EHAC and EP, was marginal compared with the value for the individual starches (369 vs. 358 and 286 vs. 256 g m^{-2} day^{-1}, respectively). The different PEG-based plasticizers were

not compatible with all starches; adding 20 pph of PEG1000 or PEG2000 to starch HWC, resulted in WVTR values of 471 and 245 g m^{-2} day^{-1} compared with 321 g m^{-2} day^{-1} for unplasticised HWC. The addition of 20 pph glycerol or sorbitol to HWC reduced the WVTR to 94 and 85 g m^{-2} day^{-1}, respectively. Finally the use of the less polar plasticizer, triacetin, provided a WVTR of 133 g m^{-2} day^{-1}.

The effect of bentonite loading was explored where the CNa content in a HWC-glycerol formulation was reduced from 48 to 36 to 24 pph. This caused a steady increase in the WVTR values from 34 to 46 to 56 g m^{-2} day^{-1}. Therefore, all samples were prepared by applying two wet 50 µm thick layers which had a uniform bentonite content of 48 pph (ca. 28 %mass), based on starch (standard formulation; Table 1). Increasing the thickness of the wet coated layer improved the barrier properties of the coating (lower WVTR values) as a result of increased coat weight after drying. For example, the first 50 µm layer, of a wet film of the standard formulation, HWC-CNa-PEG600 (20), provided a dry coat weight of 6 - 8 g m^{-2} (8 - 9 µm) and a WVTR of 35 g m^{-2} day^{-1}. The second 50 µm layer resulted in a total dry coat weight of 11 - 13 g m^{-2} (16 - 17) µm and reduced the WVTR to 18 g m^{-2} day^{-1}. Applying three or four layers further reduced the WVTR values, which levelled off at 15 ± 1 g m^{-2} day^{-1}, making the marginal gain in barrier properties unattractive compared with the potential for increased process time and cost.

The WVTR results for starch-coated paper (Fig. 1a) and paper coated with starch and bentonite (Fig. 1b) showed that the bentonites divided into two distinct groups. Adding the bentonites PGV and N116 to any of the starches resulted in higher WVTR values than starch alone indicating that these bentonites interfered with the film forming properties of the starch. In sharp contrast, the formulations containing CNa and PGN significantly improved the moisture barrier properties of all four starches. The behaviour of these two sets of bentonites aligned with the different charge characteristics in that the better barrier properties were obtained when the lower charge bentonites, CNa and PGN, were incorporated in the coating. The lowest WVTR value, 66 g m^{-2} day^{-1}, was obtained with EHAC-CNa. This observation is

presumably attributed to a higher crystallinity related to its higher amylose content because the bentonite does not associate itself with the crystalline regions, but is dispersed in the amorphous regions through which diffusion occurs. Consequently, the amount of bentonite in the amorphous regions of EHAC is higher than the nominal 28.5 %mass that is added to the formulation.

Fig. 1b and 1c demonstrates that adding PEG600, to the starch plus bentonite matrix, significantly improved the water vapour barrier properties of the coating; for example, adding 20 pph PEG600 to EHAC-N116 reduced the WVTR from 592 to 147 g m^{-2} day^{-1}. In some cases the bentonite can act as a compatibiliser (Yurelki *et al*., 2003; Wang *et al*., 2003); coercing particular combinations of starch and plasticizer (e.g. HWC + PEG600) to produce a coherent coating, an outcome that could not be accomplished in the absence of bentonite. Those coatings containing CNa generally provided the lowest WVTR values reaching 18 g m^{-2} day^{-1} for HWC-CNa-PEG600(20) (Fig. 1c).

Starch HWC was selected for a more extensive investigation because it had favourable viscosity/processing characteristics, produced fewer bubbles in the coating and contributed to the lowest WVTR in combination with all four clays. Extensive experimentation also established that this formulation was the most robust towards modification/optimisation.

Combining CNa with starch HWC and the optimised quantity of PEG600, triacetin, sorbitol or glycerol (Fig. 2) resulted in WVTR values < 50 g m^{-2} day^{-1}, which were much lower than starch alone or starch and plasticizer without bentonite (Fig. 1a). Corresponding coatings containing starch EHAC were distinctly competitive, but those based on EP provided a poorer barrier. There were subtle differences between samples containing different amounts of PEG600, PEG1000 and PEG2000 (not illustrated), but excellent values of 12 ± 2 g m^{-2} day^{-1} were obtained at concentrations ≥ 20 pph (Fig. S5).

There was a strong correlation between the barrier properties of a particular film and the amount of plasticizer present. The most pertinent example is that of sorbitol in HWC (Fig. 2a)

in that the WVTR value decreased markedly as the amount of d-sorbitol in the coated film increased and a competitive barrier (WVTR = 10 g m^{-2} day^{-1}) required 30 pph. The amount of glycerol added to HWC-CNa exerted less influence on the WVTR values. The WVTR values for EHAC-CNa-glycerol and EP-CNa-glycerol were not competitive. The combination of the different plasticizers plus CNa in the starches EC, HWC and EHAC (Fig. 2a) reinforced the need for compatibility between different combinations of starch and plasticizer. For example, increasing the triacetin content to 30 pph in HWC improved the WVTR value reaching 27 g m^{-2} day^{-1} (Fig. 2b) although this value was disappointing compared with the other, much lower values in Fig. 2.

3.2 X-Ray Diffraction studies of samples cast on glass slides

Swelling clay minerals are particularly useful when probing coatings because the values obtained for the d-values provides useful information concerning the location of at least some of the components present in the coating formulation.

3.2.1 Bentonite-plasticizer samples

Aliquots of the different coating formulations were dried on glass slides to obtain benchmark diffraction traces when none of the starch or plasticizer was sorbed into the paper (hence reducing the amount available to the bentonite) and to avoid diffraction reflections arising from the paper. Generally, when bentonite and plasticizer are mixed, the d_{001} value reflects the plasticizer loading. Taking the CNa-PEG600 system, at 20°C, as an example (Fig. 3a), the d_{001} value increases with the amount of plasticizer offered and levels off near 14.0 Å at PEG600 loadings of 12.5 %mass. It then undergoes a step change to 18.5 Å at ≥ 15 %mass and does not change even when 30 %mass PEG600 is offered (Figure 3b), in line with the observation by others (Chen and Evans, 2004; Chen *et al*., 2004). Note that the hydrodynamic radius of the PEG molecules varies with molecular weight and is 8 Å, 9.4 Å and 12.2 Å for PEG600, 1000 and 1500, respectively (Merzylyak *et al*., 1999), hence a 14.0 Å spacing precludes the suggested helical conformation in the interlayer space (Ruiz-Hitzky

and Aranda, 1990) and supports the general consensus that it is an extended chain in contact with the bentonite surface (Reinholdt *et al*., 2005). Clegg *et al*. (2014) have recently demonstrated that the 14.0 Å spacing is established at a relatively low PEG loading before a complete PEG monolayer is formed in the interlayer region. They also showed that at loadings above 15 %mass the higher spacing (18.5 ± 0.5 Å) intercalate is formed yet the spacing does not increase further even at loadings up to 30 %mass. This confirms that it is possible to have 'under-filled' interlayers at particular PEG loading levels. The water molecules hydrating the exchange cations in a PEG-free bentonite interlayer are relatively labile and are removed upon heating to ca. 100°C. This loss of water is accompanied by a reduction in the d_{001} spacing to 9.6-10.0 Å which reflects the closest possible approach of the bentonite layers. The presence of organic species in the interlayer space generally increases the d_{001} spacing and the temperature at which the interlayer of the resulting bentonite-organic complex collapses can be significantly higher than that of a bentonite-water system. The open symbols (Fig. 3b, d) illustrate how the d-value was stable to temperatures of 150°C provided the amount of plasticizer offered to the bentonite approached 10 %mass. Below this amount the presence of a d-value near 10 Å confirmed that neither plasticizer nor water was retained in the interlayer after heating. The X-ray diffraction profiles obtained using the low molecular weight plasticizer, sorbitol, behaved in an analogous manner (Fig. 3 c, d) confirming that this behaviour is not limited to oligomeric or polymeric plasticizers.

3.2.2 Bentonite-starch films

The difference in behaviour of the two bentonite groups, was immediately apparent in the bentonite-starch intercalates in that samples containing CNa and PGN displayed high intensity reflections with an increased spacing near 21.0 Å (Fig. 4a) which agrees with reliable published values (Dean *et al*., 2007; Chiou *et al*., 2006); whereas PGV and N116 exhibited lower intensity reflections associated with a d_{001} value of 13.4; i.e. almost identical to the as-received bentonite. Fig. S6a to S6d illustrate that both pairs of bentonites behaved

in a similar manner with all four starches. Fig. 4b confirmed that upon heating the HWC-PGV sample to 100°C the reflection at 6.9 °2θ was shifted to near 11 Å unequivocally confirming that no starch had been present in the interlayer of PGV, whereas the d-value of the HWC-CNa sample only underwent a minor contraction upon heating. The HWC-PGN and HWC-N116 samples behaved in an identical manner to the HWC-CNa and HCW-PGV samples, respectively. This firmly established that, at the quantities made available to the bentonites with a layer charge > 0.4 electrons per formula unit, PGV and N116, were not able to accommodate starch in the interlayer space whereas CNa and PGN could do so. Dean *et al*. (2007) noted the reluctance of a synthetic mica, of high cation exchange capacity, to expand with high amylose corn starch when mixed in a twin screw extruder whereas CNa expanded to 20 Å under the same conditions.

Masclaux and co-workers (Masclaux *et al*., 2010) referred to the ability of a plasticizer to increase the mobility of the starch molecules within a coating or film and explained how this mobility is reduced when starch is adsorbed on a bentonite. In the next section the current study is extended to consider the complex interplay between bentonite, starch and plasticizer.

3.2.3 Starch-bentonite-plasticizer films

Fig. 5 and S6 e-f show that when any of the four bentonites were mixed with both starch and 20 pph PEG600, a well-ordered, intercalated system, with a d_{001} of 19.0 ± 0.2 Å was always formed. The higher order reflections (002, 003, 004, 005, 006) present, demonstrate that the bentonite layers were more ordered when PEG600 was present in the starch coating. Indeed, the diffraction traces were almost identical to those for CNa with high PEG600 loadings (Fig. 3; in which 30 %mass of plasticizer is equivalent to 42 pph). Increasing the PEG molecular weight from 600 to 1000 to 2000 had little effect on the starch-bentonite-plasticizer spacing (19.0 Å), or d_{001} intensity, at plasticizer loadings of 10, 20 and 30 pph (not illustrated).

This behaviour, a rational series of 001 reflections associated with a d-value near 19.0 Å has prompted several workers to state that plasticizers, such as glycerol and sorbitol, are adsorbed in preference to starch (de Carvalho *et al*., 2001; Chivrac *et al*., 2008; Chivrac *et al*., 2010a,b; Souza *et al*., 2012; Wilhelm *et al*., 2003). However, a d-value of 19.0 Å does not exclude the possibility that starch and plasticizer simultaneously occupy the same interlayer. The intensity of the 001 reflections from the films cast using PGV and N116 was less than half that of the corresponding reflections for the films cast using CNa and PGN. This marked difference suggests that the bentonite platelets in the starch-PEG600 films prepared using PGV and N116 were not as well ordered as those containing CNa and PGN. Recalling that PGV and N116 were unable to accommodate starch in the interlayer space may mean that the lower intensity reflections occur because considerable quantities of non-intercalated starch are present. This non-intercalated starch may interfere with the ordering of the bentonite platelets resulting in weaker reflections. Indeed, scanning electron micrographs (Section 3.4 below) indicated that this excess starch may result in the starch-bentonite-plasticizer films fracturing parallel to the surface of the bentonite particles.

It is evident that those formulations where starch may be accommodated in the bentonite interlayer offer superior barrier properties. Bentonites with layer charges < 0.4 electrons per formula unit can accommodate starch in the interlayer, resulting in strong bentonite-starch interactions and increased d-values. Whereas bentonites with higher layer charges per formula unit do not intercalate starch, in the absence of plasticiser, and are thus considered to form bentonite-plasticizer aggregates dispersed in a starch or starch-plasticizer matrix rather than intercalated starch-bentonite composites. This type of microcomposite is likely to display weaker mechanical properties because the poor dispersion of the individual bentonite layers will severely limit the number of bentonite-starch interactions which are the origin of enhanced mechanical properties. In the barrier coatings under consideration here the ability of the bentonite to accommodate both starch and plasticizer in the interlayer appears to be a prerequisite to obtain the lowest WVTR values. This may result from the

formation of a more coherent film because of the more even distribution of starch and plasticizer between the matrix and the bentonite component rather than an assemblage of (large) bentonite-plasticizer aggregates in a starch matrix (*vide infra*).

3.3 X-ray diffraction data for coated paper samples

3.3.1 Starch-bentonite and starch-bentonite-PEG600

It is customary to apply two thin coats of any formulation onto a paper substrate in order to minimise the deceptive impact any pinholes present would have on the WVTR values determined. SEM imaging of top surfaces (data not shown) confirmed that no pinholes were present. The XRD traces for paper with two coats of starch-bentonite or starch-bentonite-plasticizer reinforced the different behaviour of the two bentonite pairs (Fig. 6).

In general, the reflections observed in the traces collected from the glass microscope slides (Fig. 5) were superimposed on those of the paper substrate (Fig. S2). Only the X-ray traces for the samples containing CNa or PGV are illustrated but are representative for those obtained using PGN and N116 (Fig. S7b and S7d, respectively). The high WVTR values recorded for samples made using PGV and N116 (Fig. 1) suggests that they adopted the bentonite-PEG microstructure in the starch-plasticizer matrix on paper. Minor differences in the position of the 001 reflection for the HWC-CNa and HWC-PGV systems (Fig. 6a and c), compared to the corresponding values from samples on glass slides (Fig. 4a), suggest subtle changes in either the bentonite dispersion and/or penetration of starch into the bentonite interlayer; perhaps reflecting the different drying routines used for glass slides and paper or the capacity of the paper to preferentially sorb starch and/or plasticizer. The 001 reflections for HWC-CNa (Fig. 6a) and HWC-PGN (Fig. S7b) were more intense (compare the intensity of the reflection at 4.7 °2θ, Fig. 6, with that arising from the paper near 22 °2θ) than those for HWC-PGV (Fig. 6b) and HWC-N116 (Fig. S7d). This suggests that the coatings containing PGV and N116 led to films with ordered bentonite on paper but those films did not cover the fibres as well and/or the ordered domains were not as extensive;

perhaps due to the presence of non-intercalated starch. This observation correlated strongly with the WVTR data (Fig. 1) in that the coatings containing PGV and N116 exhibit significantly poorer barrier properties.

The addition of plasticizer to the starch-bentonite matrix (Fig. 6c, 6d) resulted in a sharper, more intense 001 reflection for each coating system; as observed in the films coated on glass slides (Fig. S7 e-h). Nevertheless, the intensities of the 001 reflections arising from the starch-plasticizer samples containing PGV and N116 were considerably weaker than those exhibited by those containing CNa and PGN. This further reinforces both the contribution that the plasticizer makes to the ordering of the bentonites in their individual coatings and the division of the four bentonites into two distinct groups.

3.3.2 Starch-bentonite samples plasticised with triacetin, glycerol, and sorbitol.

The HWC-CNa-triacetin systems, dried on paper (Fig. 7a) were the most similar to the corresponding PEG-containing samples (Fig. 6c) in that the 001 reflection was considerably more intense than the diffraction peaks from the paper substrate. However, the d-values were lower at 17.0 Å and the WVTR value was comparatively high at 33 ± 5 g m^{-2} day^{-1}. The XRD traces from the HWC-CNa-glycerol system dried on paper (Fig. 7b) displayed an 001 reflection (21.0 Å) that was two times less intense than those exhibited by the corresponding HWC-CNa coating containing PEG600 (Fig. 6c). Nonetheless, the coatings containing 20 and 30 pph glycerol provided WVTR values of ≤ 13 g m^{-2} day^{-1} (Fig. 1).

The XRD traces, collected from samples coated on paper (Fig. 7c), confirmed that the HWC-CNa-sorbitol formulations produced less well ordered systems with a higher d_{001}-spacing (21 Å) than the corresponding samples prepared using PEG or triacetin. Since the XRD trace for CNa with 30 pph sorbitol alone (Fig. 3c) exhibited a series of well-ordered basal reflections commensurate with a spacing of 19.0 Å, it is hypothesised that the comparatively broad, 21.0 Å reflection indicated that both starch and sorbitol reside in the same interlayers. The

HWC-CNa-sorbitol(30) provided a WVTR of 10 g m^{-2} day^{-1}. The XRD traces from samples coated on glass and on paper are compared in Fig. S8.

3.4 Electron microscopy of freeze fractured, cast films

The scanning electron micrographs for CNa-PEG600(63), i.e. 63 pph PEG600 relative to 100 pph CNa, clearly illustrated a layered structure (Fig. 8a) as did CNa-triacetin(63) (Fig. 8b). Both of these samples contain 61 %mass of CNa. At higher magnification (Fig. 8c) the undulations in the CNa-PEG600(63) film were more apparent as was the observation that the layers were considerably thicker than the 1 nm associated with an individual bentonite layer. The decreased bentonite content in the micrographs for HWC-CNa (32 %mass CNa; Fig. 8d) and HWC-CNa-PEG600(20) (28 %mass CNa; Fig. 8e) resulted in a less densely packed structure but once again the layers on view were considerably thicker than 1 nm. Hence, the ca. 60 nm thickness (±10 nm as measured using SEM) of these macroscopic layers, a representative selection of which is provided in the four micrographs (Fig 8a, 8c, 8d and 8e), was the same even though the bentonite/organic ratios were not identical. Finally, layers of the same thickness were clearly visible in the HWC-CNa-PEG600(20) coating on paper (Fig. 8f).

Malwitz and co-workers (Malwitz *et al*., 2003) were the first to report the presence of a reflection arising from a 60 nm layer in the SANS data for dried PEG films containing 15 %mass, 40 %mass and 60 %mass Laponite® and they also observed a similar reflection in a PEG film containing 40 %mass CNa. First Dundigalla *et al*. (2005) and then Stefanescu *et al*. (2006) presented AFM images of fractured cross sections which confirmed the presence of these layers and that they were formed of linear assemblies of elliptical 'globules', measuring ca. 30-60 nm x 60 nm (x-axis length x height) for Laponite® RD-based and ca. 100 nm x 60 nm for CNa-based layers, both resulting in a striped texture. The effect was more apparent in samples where at least 60 %mass of Laponite® was incorporated in high molecular weight polyethylene oxide, PEO ($1x10^6$). It is crucial to note that the globules

which join up to form these 60 nm thick linear assemblies, termed supramolecular layers by the authors, are not present in the precursor suspension (Loizou *et al*., 2005, 2006). Scattering results unequivocally prove that the Laponite® particles exist as individual, dispersed, polymer coated layers in the precursor suspension in agreement with the work of others (Nelson and Cosgrove, 2004). The supramolecular layers identified by Dundigalla *et al*. (2005) and Stefanescu *et al*. (2006) were clearly present in their micrographs of samples containing 60 %mass bentonite, but were much less evident when the bentonite content decreased to 40 and 15 %mass. The formation of these supramolecular layers was attributed to the orientation of the bentonite particles combined with the stretching of the polymer chains that occurs during the film spreading and subsequent drying. A schematic illustration of the different suggested structures within the 60 nm globules, proposed to exist in this study, and how they could combine to form the supramolecular layers in the coatings prepared using starch-bentonite-plasticizer mixtures is presented in Fig. 9.

Close scrutiny of multiple SEM images suggested that the formulations containing PGV and N116 fractured parallel to the surface of the supramolecular layers whereas those containing CNa and PGN fractured perpendicular to the 60 nm thick layers. One interpretation of this marked difference in fracture mechanism is that the excess, unattached starch in the coating matrix, which PGV and N116 were unable to accommodate in the interlayer space (Fig. 4), caused fracture to progress parallel to the film surface and not perpendicular to it. Stefanescu *et al*. (2006) reported that intercalated CNa-PEG(67) nanocomposites fractured perpendicular to the supramolecular layers whereas samples prepared using Laponite® fractured parallel to the supramolecular layers.

4. Discussion

The results clearly demonstrate that the type of plasticizer exerts a significant effect on the WVTR values of the bentonite-free starch coatings (Fig. 1a). Adding PEG600 did little to improve the barrier properties of starches EHAC and EP whereas its poor compatibility with

EC and HWC produced incoherent coatings with unacceptable barrier properties. Increasing the molecular weight of the PEG used had no appreciable effect on the barrier properties of HWC whereas the incorporation of sorbitol, glycerol or triacetin served to reduce the WVTR properties of the coated paper.

The profound effect of incorporating 48 pph (28 %mass) of the lower layer charge bentonites was evident in all samples containing CNa and PGN and was even more pronounced when a plasticizer was included in the formulation (Fig. 1b). Even though the final WVTR values achieved using CNa and PGN were the lowest, the result of combining the less effective, higher charge bentonites, PGV and N116, with PEG600 was equally dramatic; the WVTR dropped almost five fold from 700 g m^{-2} day^{-1} (HWC-PEG600 coated paper) to 150 g m^{-2} day^{-1}. Nonetheless, as Fig. 2 clearly illustrates the lowest WVTR values required the optimisation of all three components. In this study, the preferred combination was starch HWC, CNa and PEG600. Some combinations of EC, plasticizer and CNa offer competitive WVTR values but extensive experimentation with starch HWC has conclusively demonstrated that this matrix was the most robust overall.

In a recent review Tan and Thomas (2016) concluded that the percentage reduction in water vapour permeability, WVP, resulting from the addition of bentonite nanoparticles is largely independent of polymer type. They attributed the reduction in WVP to the filler type (raw clay or organomodified bentonite) and concentration. The aspect ratio is also a significant consideration when the clay mineral addition levels are below 5 %mass above which layer-layer aggregation must occur. The review focussed on polymer films rather than coatings and few examples of water-soluble polymers were presented. Nonetheless, reductions in WVP of > 90% were achieved at bentonite loadings of 15 %mass in polycaprolactone, PCL (Gorassi *et al*., 2002), 30 %mass in polybenzimidazole, PBI (Karthikeyan *et al*., 2006), and 40 %mass in polyurethane, PU (Tortora *et al*., 2002), all of which were prepared by casting from suitable solvents. More appropriate comparisons are available with self-supporting, thermoplastic starch films. Park *et al.* (2002) reported a 50% reduction in the water vapour

permeability, at 54 %RH and 24°C, after adding 5 %mass clay to a mixture of 100 pph potato starch plus 60 pph glycerol. Muller *et al*. (2011) reported a similar reduction in WVP, albeit under more demanding conditions of 75% RH and 25°C, after adding 5 %mass montmorillonite to a 100 pph cassava starch plus 25 pph glycerol matrix. Tang *et al.* (2008a,b) were only able to reduce the WVP by 55% at 75% RH and 25°C by incorporating 9 %mass montmorillonite in a 100 pph potato starch plus 15 pph glycerol. Ning *et al.* (2009) also reduced the WVP by 60 % at 75%RH and 24°C when they dispersed 9% of a chinese montmorillonite in corn starch and glycerol (30%). All the preceding data for starch nanocomposites was obtained using self-supporting films of 100 to 500 μm thickness prepared using melt compounding approaches and thus are not the ideal comparators for the coated, low basis weight paper used in this study. Schumann *et al.* (2005) noted that the WVTR of a styrene-butadiene (SB) latex on a 160 g m^{-2} paper board was 28 g m^{-2} day^{-1} at 50% RH and 24°C and this could be almost halved to 15 g m^{-2} day^{-1} if 60 %mass of the non-expanding clay minerals, kaolin or talc, were mixed into the SB latex. Unlike starch the SB latex is organophilic and offers a better barrier to water vapour which is why the initial value is so low at 28 g m^{-2} day^{-1}. The authors normalised the WVTR values to a 10 μm coating thickness which means that the final value of 15 g m^{-2} day^{-1} can be compared directly with the values in Fig. 1 and 2. Thus, Schumann *et al.* (2005) were able to reduce the water vapour transfer rate by a factor of 2 with a high loading of non-expanding clay (kaolin).

The data in Fig. 2, and earlier published work using starch-CNa-PEG400(30) (Johansson *et al*., 2010; Olsson *et al*., 2014a,b), shows that the addition of 32.4 %mass of the bentonites capable of adsorbing starch into the interlayer (CNa, PGN) reduced the WVTR by a factor of 3 from ca 340 ± 20 g m^{-2} day^{-1} to 70 to 120 g m^{-2} day^{-1}, whereas the higher charge bentonites (PGV, N116), which did not adsorb the starch, interfered with the starches' natural film forming properties and returned very poor barrier properties (400 - 600 g m^{-2} day^{-1}). The reduction in WVTR was more marked here (Fig. 1, 2) than in earlier studies where the application of two layers of starch-CNa-PEG400(30) reduced the WVTR value of the

uncoated, low basis weight, waxed paper from 119 to 21.2 g m^{-2} day^{-1} (Olsson *et al*., 2014a). The final values of WVTR obtained using the more impermeable, starch-bentonite coatings clearly demonstrate that incorporation of the optimised quantity of plasticizer, provided WVTR values directly comparable to those of the 'hydrophobic' SB latex. This reinforces the view that the synergistic behaviour exhibited by the optimised starch-bentonite-plasticizer mixtures made them competitive with industry standard barrier latexes when compared at similar temperatures and % RH (Olsson *et al*., 2014a,b).The overarching result is that a combination of both the bentonite and plasticizer in a starch coating acted in a synergistic manner to significantly improve the water vapour barrier properties even when addition of either of the individual components significantly diminished the barrier properties, e.g. compare HWC (321 g m^{-2} day^{-1}) with HWC-PGV-PEG600 (79 g m^{-2} day^{-1}), HWC-PEG600 (673 g m^{-2} day^{-1}) and HWC-PGV (425 g m^{-2} day^{-1}) or compare HWC (321 g m^{-2} day^{-1}) with HWC-N116-PEG600 (87 g m^{-2} day^{-1}), HWC-PEG600 (673 g m^{-2} day^{-1}) or HWC-N116 (520 g m^{-2} day^{-1}), (Fig. 1 and 2).

There were significant differences in the way that bentonites influence the WVTR properties of starch-plasticizer films (Fig. 1) in that the best water vapour barrier properties were obtained in the bentonite systems that were intercalated with starch (CNa and PGN; Fig. 1c), whereas the worst were with those in which a microcomposite of bentonite-PEG600 in a starch:PEG matrix was formed (PGV and N116; Fig. 1c). The surmised presence of a starch-plasticizer phase surrounding the plasticizer intercalated bentonite in the microcomposite structure present in the coatings containing N116 and PGV introduces the probability of interconnected, bentonite-poor channels, of unspecified composition, which provide rapid transfer routes for water. Consequently, the high WVTR values for the N116 and PGV containing formulations (Fig. 1) are considered to reflect the presence of these low barrier channels (Fig. 9b). In order to illustrate the velocity at which water can negotiate such a rapid transfer route, the lowest WVTR for a bentonite free coating (85 g m^{-2} day^{-1}) was achieved with a mixture of 100 pph HWC and 20 pph of sorbitol.

Several different coatings systems have been prepared that exhibit very good water vapour barrier properties and as shown in the data these are mainly dependent on the type of starch, and type or concentration of plasticizer. The example of triacetin plus bentonite in the starches EC, HWC and EHAC (Fig. 2b) clearly suggests that the compatibility of different starches with a given plasticizer also has a role to play. Two further examples include the EHAC-CNa-sorbitol(30) and EC-CNa-PEG600(20) systems, which gave WVTR values of 9 and 10 g m^{-2} day^{-1}, respectively.

It is generally accepted that the average platelet dimensions of the individual bentonites should also be considered particularly since Bharadwaj (2001) has demonstrated that bentonites with larger diameters are more forgiving of (small) variations in alignment whereas bentonites with smaller diameters need to be better aligned to provide a comparable barrier. However, his calculations focussed on relatively low loadings of bentonite in the matrix and did not consider the influence of loadings as high as those used here nor did it consider the presence of the supramolecular layers.

5. Conclusions

This study has shown that bentonite can be used to significantly improve the moisture barrier properties of sustainable starch coatings for paper and board reducing the water vapour transmission rate (WVTR) of the base paper from 780 to ≤ 10 g m^2 day^{-1} for the optimised starch-bentonite-plasticizer coating formulation. It has demonstrated that bentonites with a layer charge of < 0.4 electrons per formula unit were able to accommodate starch in the interlayer space and, when incorporated in the coating, routinely provided the highest barrier to water vapour. In contrast, bentonites with a layer charge of > 0.4 electrons per formula unit were not able to accommodate starch in the interlayer space and WVTR values for comparative coatings, prepared using the higher charge bentonites, were three to four times higher (35 ± 7 g m^2 day^{-1}).

The addition of bentonite ensures formation of coherent films and coatings even when the starch and plasticizer are incompatible in the absence of bentonite. This ability does not appear to depend on the layer charge of the bentonite.

Scanning electron micrographs provided clear evidence for the presence of 60 nm thick supramolecular layers formed from starch-bentonite-plasticizer in the samples coated on glass and paper.

The WVTR values for these low-eco footprint coatings are competitive with proprietary coatings prepared using petroleum derived resins.

Acknowledgements

This work was funded under the 7th Framework Programme of the European Union "FLEXPAKRENEW – Design and Development of an innovative, eco-efficient, low substrate flexible paper packaging from renewable resources to replace petroleum based barrier films". Grant agreement number NMP3-SL-2008-207810.

References

Bharadwaj, R.K., 2001. Modelling the barrier properties of polymer-layered silicate nanocomposites. Macromolecules 34, 9189-9192.

Breen, C., Zahoor, F.D., Madejova, J., Komadel, P. 1997 Characterisation and Catalytic Activity of Acid Treated, Size-fractionated Smectites. Journal of Physical Chemistry B. 1101:5324-5331.

Buzby, J.C., Hyman, J., 2012. Total and per capita value of food loss in the United States. Food Policy 37, 561-570.

Chen, B., Evans, J., 2005. Thermoplastic starch-clay nanocomposites and their characteristics. Carbohydr. Polym. 61, 455-463.

Chen, B., Evans, J., 2004. Preferential intercalation in polymer-clay nanocomposites. J Phys Chem B 108, 14986-14990.

Chen, B., Evans, J., Holding, S., 2004. Decomposition of poly(ethylene glycol) in nanocomposites. J Appl Polym Sci 94, 548-552.

Chiou, B., Yee, E., Wood, D., Shey, J., Glenn, G., Orts, W., 2006. Effects of processing conditions on nanoclay dispersion in starch-clay nanocomposites. Cereal Chem. 83, 300-305.

Chivrac, F., Pollet, E., Averous, L., 2010a. Shear induced clay organo-modification: application to plasticized starch nano-biocomposites. Polym. Adv. Technol. 21, 578-583.

Chivrac, F., Pollet, E., Dole, P., Averous, L., 2010b. Starch-based nano-biocomposites: Plasticizer impact on the montmorillonite exfoliation process. Carbohydr. Polym. 79, 941-947.

Chivrac, F., Pollet, E., Schmutz, M., Averous, L., 2010c. Starch nano-biocomposites based on needle-like sepiolite clays. Carbohydr. Polym. 80, 145-153.

Chivrac, F., Pollett, E., Schmutz, M., Averous, L., 2008. New approach to elaborate exfoliated starch-based nanobiocomposites. Biomacromolecules 9, 896-900.

Choudalakis, G., Gotsis, A.D., 2009. Permeability of polymer/clay nanocomposites: A review. European Polymer Journal 45, 967-984.

Christidis, G.E., Eberl, D.D., 2003. Determination of layer-charge characteristics of smectites. Clays Clay Miner. 51, 644-655.

Chung, Y., Lai, H., 2010. Preparation and properties of biodegradable starch-layered double hydroxide nanocomposites. Carbohydr. Polym. 80, 525-532.

Clegg, F., Breen, C., Khairuddin, 2014. Synergistic and Competitive Aspects of the Adsorption of Poly(ethylene glycol) and Poly(vinyl alcohol) onto Na-Bentonite. J Phys Chem B 118, 13268-13278.

de Carvalho, A., Curvelo, A., Agnelli, J., 2001. A first insight on composites of thermoplastic starch and kaolin. Carbohydr. Polym. 45, 189-194.

Dean, K.M., Do, M.D., Petinakis, E., Yu, L., 2008. Key interactions in biodegradable thermoplastic starch/poly(vinyl alcohol)/montmorillonite micro- and nanocomposites. Composites Sci. Technol. 68, 1453-1462.

Dean, K., Yu, L., Wu, D.Y., 2007. Preparation and characterization of melt-extruded thermoplastic starch/clay nanocomposites. Composites Sci. Technol. 67, 413-421.

Donnadio, A., Pica, M., Taddei, M., Vivani, R., 2012. Design and synthesis of plasticizing fillers based on zirconium phosphonates for glycerol-free composite starch films. J. Mater. Chem. 22, 5098-5106.

Dundigalla, A., Lin-Gibson, S., Ferreiro, V., Malwitz, M., Schmidt, G., 2005. Unusual multilayered structures in poly(ethylene oxide)/laponite nanocomposite films. Macromolecular Rapid Communications 26, 143-149.

Ebina, T., Mizukami, F., 2007. Flexible transparent clay films with heat-resistant and high gas-barrier properties. Adv Mater 19, 2450-+.

European Commission, 2016. Food Waste report for EU. http://ec.europa.eu/food/safety/food_waste/index_en.htm (accessed 27th January 2019).

Findenig, G., Leimgruber, S., Kargl, R., Spirk, S., Stana-Kleinschek, K., Ribitsch, V., 2012. Creating Water Vapor Barrier Coatings from Hydrophilic Components. ACS Applied Materials & Interfaces 4, 3199-3206.

Gorrasi, G., Tortora, M., Vittoria, V., Galli, G., Chiellini, E. 2002. Transport and mechanical properties of blends of poly(ε-caprolactone) and a modified montmorillonite- poly(ε-

caprolactone) nanocomposite. Journal of Polymer Science. Part B. Polymer Physics. 40, 1118–1124.

Isayama, M., Kunitake, T., 1994. Self-supporting films of clay minerals and metal oxides: Molecular ceramics. Advanced Materials, 6, 77-78.

Johansson, C., Bras, J., Mondragon, I., Nechita, P., Plackett, D., Simon, P., Svetec, D. G., Virtanen, S., Baschetti, M. G., Breen, C. *et al.* 2012. Renewable Fibres and Biobased Materials for Packaging applications - A review of Recent Developments. Bioresources *7*, 2506-2552.

Johansson, C., Jarnstrom, L., Breen, C. 2010. Bioploymer based biomaterial and method for making the same. WO 2010/077203 A1.

Kalambur, S., Rizvi, S., 2004. Starch-based nanocomposites by reactive extrusion processing. Polym. Int. 53, 1413-1416.

Kampeerapappun, P., Aht-ong, D., Pentrakoon, D., Srikulkit, K., 2007. Preparation of cassava starch/montmorillonite composite film. Carbohydr. Polym. 67, 155-163.

Karthikeyan, C.S., Nunes, S.P., Schulte, K. 2006. Barrier properties of poly(benzimi-dazole)-layered silicates nanocomposite materials. Advanced Engineering Materials. 8, 1010–1015.

Kummu, M., de Moel, H., Porkka, M., Siebert, S., Varis, O., Ward, P.J., 2012. Lost food, wasted resources: Global food supply chain losses and their impacts on freshwater, cropland, and fertiliser use. Sci. Total Environ. 438, 477-489.

Laufer, G., Kirkland, C., Cain, A.A., Grunlan, J.C., 2012. Clay-Chitosan Nanobrick Walls: Completely Renewable Gas Barrier and Flame-Retardant Nanocoatings. ACS Applied Materials & Interfaces 4, 1643-1649.

Li, R., Liu, C., Ma, J., 2011. Studies on the properties of graphene oxide-reinforced starch biocomposites. Carbohydr. Polym. 84, 631-637.

Loizou, E., Butler, P., Porcar, L., Kesselman, E., Talmon, Y., Dundigalla, A., Schmidt, G., 2005. Large scale structures in nanocomposite hydrogels. Macromolecules 38, 2047-2049.

Loizou, E., Butler, P., Porcar, L., Schmidt, G., 2006. Dynamic responses in nanocomposite hydrogels. Macromolecules 39, 1614-1619.

Lu, P., Zhang, M., Liu, Y., Li, J., Xin, M. 2012 Characteristics of vermiculite-reinforced thermoplastic starch composite films. Journal of Applied Polymer Science 126,E116-E122.

Malwitz, M., Lin-Gibson, S., Hobbie, E., Butler, P., Schmidt, G., 2003. Orientation of platelets in multilayered nanocomposite polymer films. Journal of Polymer Science Part B-Polymer Physics 41, 3237-3248.

Masclaux, C., Gouanve, F., Espuche, E., 2010. Experimental and modelling studies of transport in starch nanocomposite films as affected by relative humidity. J. Membr. Sci. 363, 221-231.

Mbey, J.A., Hoppe, S., Thomas, F., 2012. Cassava starch-kaolinite composite film. Effect of clay content and clay modification on film properties. Carbohydr. Polym. 88, 213-222.

McGlashan, S., Halley, P., 2003. Preparation and characterisation of biodegradable starch-based nanocomposite materials. Polym. Int. 52, 1767-1773.

Merzlyak, P.G., Yuldasheva, L.N., Rodrigues, C.G., Carneiro, C.M.M., Krasilnikov, O.V., Bezrukov, S.M. 1999. Polymeric nonelectrolytes to probe pore geometry: application to the *α*-toxin transmembrane channel. Biophysical Journal 77, 3203-3033

Moeller, M.W., Handge, U.A., Kunz, D.A., Lunkenbein, T., Altstaedt, V., Breu, J., 2010. Tailoring Shear-Stiff, Mica-like Nanoplatelets. ACS Nano 4, 717-724.

Mueller, C.M.O., Laurindo, J.B., Yamashita, F., 2011. Effect of nanoclay incorporation method on mechanical and water vapor barrier properties of starch-based films. Industrial Crops and Products 33, 605-610.

Muriana, C., 2015. Effectiveness of the food recovery at the retailing stage under shelf life uncertainty: An application to Italian food chains. Waste Manage. 41, 159-168.

Nam, H., Ebina, T., Mizukami, F., 2009. Formability and properties of self-standing clay film by montmorillonite with different interlayer cations. Colloids and Surfaces A-Physicochemical and Engineering Aspects 346, 158-163.

Nelson, A., Cosgrove, T., 2004. A small angle neutron scattering study of adsorbed poly(ethylene oxide) on Laponite. Langmuir. 20, 2298-2304

Ning, W., Xingxiang, Z., Na, H., Shihe, B. 2009. Effect of citric acid nd processing on the performance of thermoplastic starch/montmorillonite nanocomposites. Carbohydrate Polymers. 76, 68-73.

Olsson, E., Johansson, C., Jarnstrom, L. 2014a. Montmorillonite for starch-based barrier dispersion coatings - Part 1: The influence of citric acid and poly(ethylene glycol) on viscosity and barrier properties. Applied Clay Science. 97-98, 160-166.

Olsson, E., Johansson. C., Larsson, J., Jarnstrom, L. 2014b. Montmorillonite for starch-based barrier dispersion coatings - Part 2: Pilot trials and PE lamination. Applied Clay Science. 97-98, 167-173.

Papargyropoulou, E., Lozano, R., Steinberger, J.K., Wright, N., bin Ujang, Z., 2014. The food waste hierarchy as a framework for the management of food surplus and food waste. J. Clean. Prod. 76, 106-115.

Park, H., Li, X., Jin, C., Park, C., Cho, W., Ha, C., 2002. Preparation and properties of biodegradable thermoplastic starch/clay hybrids. Macromolecular Materials and Engineering 287, 553-558.

Peelman, N., Ragaert, P., De Meulenaer, B., Adons, D., Peeters, R., Cardon, L., Van Impe, F., Devlieghere, F., 2013. Application of bioplastics for food packaging. Trends Food Sci. Technol. 32, 128-141.

Peelman, N., Ragaert, P., Vandemoortele, A., Verguldt, E., De Meulenaer, B., Devlieghere, F., 2014. Use of biobased materials for modified atmosphere packaging of short and medium shelf-life food products. Innovative Food Science & Emerging Technologies 26, 319-329.

Priolo, M.A., Holder, K.M., Gamboa, D., Grunlan, J.C., 2011. Influence of Clay Concentration on the Gas Barrier of Clay-Polymer Nanobrick Wall Thin Film Assemblies. Langmuir 27, 12106-12114.

Reinholdt, M.X., Kirkpatrick, R.J., Pinnavaia, T.J., 2005. Montmorillonite-poly(ethylene oxide) nanocomposites: Interlayer alkali metal behavior. J Phys Chem B 109, 16296-16303.

Rhim, J., Park, H., Ha, C., 2013. Bio-nanocomposites for food packaging applications. Progress in Polymer Science 38, 1629-1652.

Ruiz-Hitzky, E., Aranda, P., 1990. Polymer-Salt Intercalation Complexes in Layer Silicates. Adv Mater 2, 545-547.

Schlemmer, D., Angelica, R.S., Sales, M.J.A., 2010. Morphological and thermomechanical characterization of thermoplastic starch/montmorillonite nanocomposites. Composite Structures 92, 2066-2070.

Schuman, T., Karlsson, A., Larsson, J., Wikstrom, M., Rigdahl, M., 2005. Characteristics of pigment-filled polymer coatings on paperboard. Progress in Organic Coatings 54, 360-371.

Souza, A.C., Benze, R., Ferrao, E.S., Ditchfield, C., Coelho, A.C.V., Tadini, C.C., 2012. Cassava starch biodegradable films: Influence of glycerol and clay nanoparticles content on tensile and barrier properties and glass transition temperature. Lwt-Food Science and Technology 46, 110-117.

Stefanescu, E., Dundigalla, A., Ferreiro, V., Loizou, E., Porcar, L., Negulescu, I., Garno, J., Schmidt, G., 2006. Supramolecular structures in nanocomposite multilayered films. Physical Chemistry Chemical Physics 8, 1739-1746.

Tan, B., Thomas, N.L., 2016. A review of the water barrier properties of polymer/clay and polymer/graphene nanocomposites. J. Membr. Sci. 514, 595-621.

Tang, X., Alavi, S., Herald, T.J., 2008. Barrier and mechanical properties of starch-clay nanocomposite films. Cereal Chem. 85, 433-439.

Tang, X., Alavi, S., Herald, T.J., 2008. Effects of plasticizers on the structure and properties of starch-clay nanocomposite films. Carbohydr. Polym. 74, 552-558.

Tortora, M., Gorrasi, G., Vittoria, V., Galli, G., Ritrovati, S., Chiellini, E., 2002. Structural characterization and transport properties of organically modified montmorillonite/polyurethane nanocomposites. Polymer. 43, 6147–6157.

Verghese, K., Lewis, H., Lockrey, S., Williams, H., 2015. Packaging's Role in Minimizing Food Loss and Waste Across the Supply Chain. Packaging Technology and Science 28, 603-620.

Walther, A., Bjurhager, I., Malho, J., Pere, J., Ruokolainen, J., Berglund, L.A., Ikkala, O., 2010a. Large-Area, Lightweight and Thick Biomimetic Composites with Superior Material Properties via Fast, Economic, and Green Pathways. Nano Letters 10, 2742-2748.

Walther, A., Bjurhager, I., Malho, J., Ruokolainen, J., Berglund, L., Ikkala, O., 2010b. Supramolecular Control of Stiffness and Strength in Lightweight High-Performance Nacre-

Mimetic Paper with Fire-Shielding Properties. Angewandte Chemie-International Edition 49, 6448-6453.

Wang, Y., Zhang, Q., Fu, Q., 2003. Compatibilisation of immisicible poly(propylene)/polystyrene blends using clay. Macromol. Rapid. Commun. 24, 231-235.

Hlavatsch, J., Wechselberger, D., Ruf, F., 1997. Streichbentonite – Neuentwicklung mit Perspektive. Wochenblatt Papierfabr. 125, 588-594.

Wikstrom, F., Williams, H., Verghese, K., Clune, S., 2014. The influence of packaging attributes on consumer behaviour in food-packaging life cycle assessment studies - a neglected topic. J. Clean. Prod. 73, 100-108.

Wilhelm, H., Sierakowski, M., Souza, G., Wypych, F., 2003. Starch films reinforced with mineral clay. Carbohydr. Polym. 52, 101-110.

Yurelki, K., Karim, A., Amis, E.J., Krishnamoorti R., 2003 Influence of layered silicates on the phase-separated morphology of PS-PVME blends. Macromolecules. 36, 7256-7267.

Tables and Figures

Table 1: Concentrations of starch, bentonite and plasticizer used in the coatings. To prepare the formulation the stated quantities of starch, bentonite and plasticizer were mixed with [a]46.3g, [b]52.3 g and [c]3g water, respectively. Hence, the value for the [d]%mass solids in the coating suspension is obtained using the total weight of solids in grams and the total amount of water used (i.e. 101.6g). Note that the standard formulation contains 100 pph of starch, 48 pph of bentonite and 20 pph of plasticizer.

Figure 1: WVTR results for paper coated with two layers of (a) pure starches and starches with 20 pph of selected plasticizers, (b) starch coatings prepared using only 48 pph of the four different bentonites or the same quantities of bentonite, but also with 20 pph PEG 600. The data presented in (c) shows in more detail the values obtained from starch-bentonite-PEG600 mixtures. NC means the non-coated paper. The numerical values represent the average of 3 WVTR measurements and the error bars represent the standard deviation of the WVTR value for a particular coating. The absent bar represented by 'X' denotes data not obtained for this sample.

Figure 2: The effect of (a) the type and amount of plasticizer on the WVTR values when used in conjunction with CNa and the starches HWC, EHAC and EP and (b) the amount of triacetin on the WVTR values for formulations containing CNa and starches EC, HWC and EHAC. The numerical values represent the average of 3 WVTR measurements and the error bars represent the standard deviation of the WVTR value for a particular coating.

Figure 3: The effect of plasticizer loading on the X-ray diffraction traces for (a) CNa-PEG600 and (c) CNa-sorbitol together with the associated d-values at 20°C and after heating to 150°C for (b) CNa-PEG600 and (d) CNa-sorbitol. In these samples the numbers associated with selected reflections are in %mass and 30 %mass is equivalent to 42 pph.

Figure 4: A comparison of the X-ray diffraction traces obtained for coatings prepared on glass slides and subsequently kept at room temperature (RT) or further dried at 100°C, (a) the bentonites PGN, N116, CNa, and PGV after mixing with starch HWC and (b) for the bentonites CNa and PGV after mixing with starch HWC and kept at room temperature or subsequent to heating at 100°C. All samples were prepared using 11.5 g starch and 5.5 g bentonite (Table 1).

Figure 5: Comparison of X-ray diffraction profiles for the starch-bentonite-plasticizer formulations identified. Samples were prepared on glass slides.

Figure 6: XRD traces obtained from paper samples coated with formulations containing (a) CNa plus starches HWC, EC, EP and EHAC, (b) PGV plus starches HWC, EC, EP and EHAC, (c) samples in (a) but with 20 pph PEG600, (d) samples in (b) but with 20 pph PEG600. P denotes a diffraction reflection from the paper substrate.

Figure 7: X-ray diffraction traces for samples of (a) CNa-HWC-triacetin (b) CNa-HWC-glycerol paper and (c) CNa-HWC-sorbitol coated on paper. Plasticizer contents were 10, 20 and 30 pph. P denotes a reflection arising from the paper substrate.

Figure 8: Scanning electron micrographs of fractured surfaces of (a) CNa-PEG600(63), (b) CNa-triacetin(63), (c) CNa PEG600(63), (d) HWC-CNa, (e) HWC-CNa-PEG600(20), and (f) HWC-CNa-PEG600(20) on paper.

Figure 9: Schematic illustration of the different structures adopted by bentonites of lower (a) and higher (b) charge in the starch-bentonite-plasticizer globules and how they contribute to the observed 60 nm thick supramolecular layers (c).

Table 1: Concentrations of starch, bentonite and plasticizer used in the coatings. To prepare the formulation the stated quantities of starch, bentonite and plasticizer were mixed with [a]46.3g, [b]52.3 g and [c]3g water, respectively. Hence, the value for the [d]%mass solids in the coating suspension is obtained using the total weight of solids in grams and the total amount of water used (i.e. 101.6g). Note that the standard formulation contains 100 pph of starch, 48 pph of bentonite and 20 pph of plasticizer.

Plasticizer content / pph	**Solids content expressed in units of**	**Amount of starch**	**Amount of bentonite**	**Amount of plasticizer**	**Solids in coating suspension/ %mass**
10	g	11.5[a]	5.5[b]	1.15[c]	15.2[d]
	pph	100	48	10	
	%mass	63.4	30.3	6.4	
20 Standard formulation	g	11.5[a]	5.5[b]	2.3[c]	16.0[d]
	pph	100	48	20	
	%mass	59.6	28.5	11.9	
30	g	11.5[a]	5.5[b]	3.45[c]	16.8[d]
	pph	100	48	30	
	%mass	56.2	26.9	16.9	
Reference coatings					
Pure starch	g	11.5[a]	0	0	19.9[d]
	pph	100	-	-	
	%mass	19.9	-	-	
Starch plus bentonite	g	11.5[a]	5.5[b]	0	14.7[d]
	pph	100	48	0	
	%mass	67.6	32.4	-	
Starch plus plasticizer (20 pph)	g	11.5[a]	0	2.3[c]	21.8[d]
	pph	100	-	20	
	%mass	83.3	-	16.7	

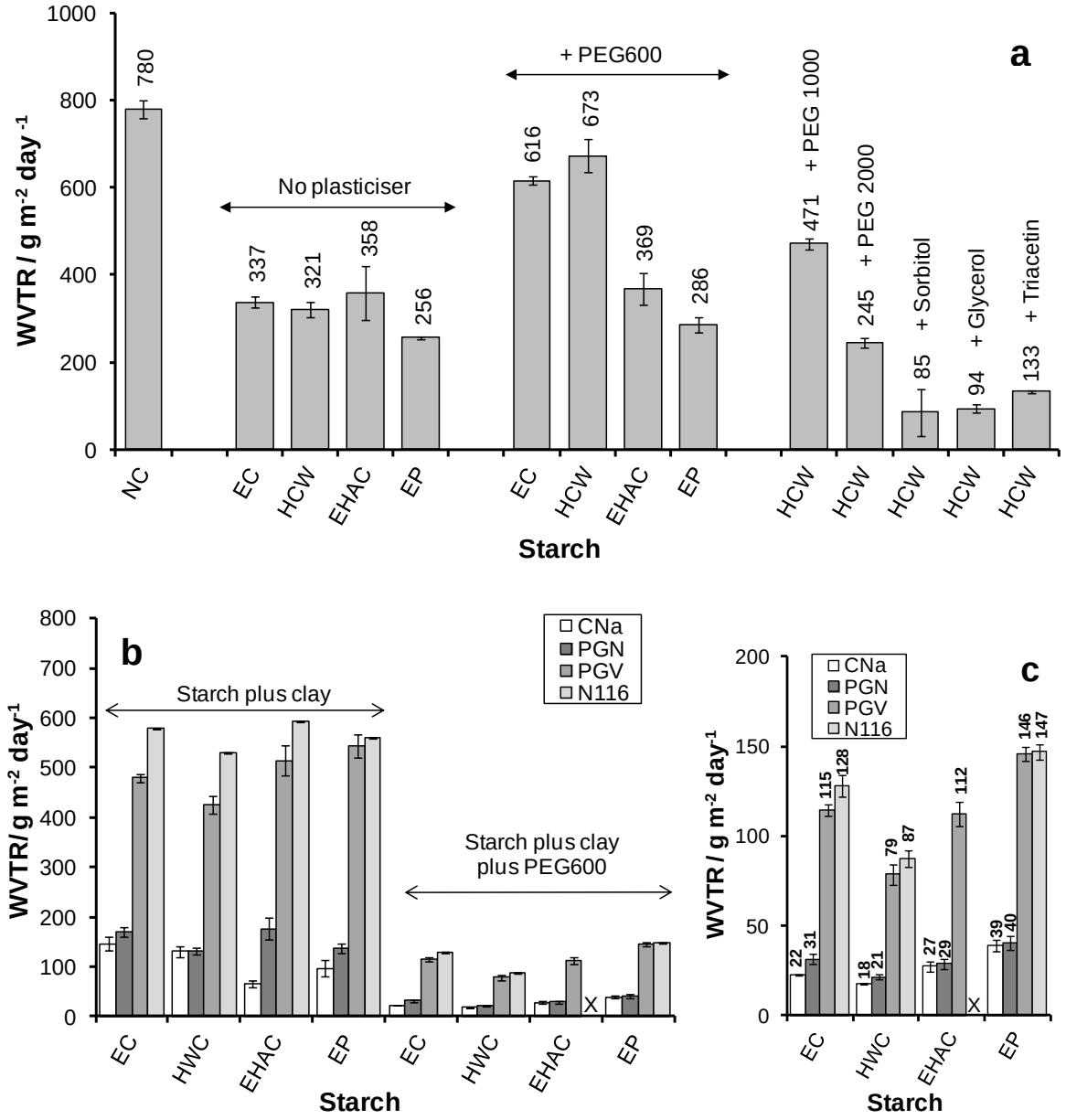

Figure 1: WVTR results for paper coated with two layers of (a) pure starches and starches with 20 pph of selected plasticizers, (b) starch coatings prepared using only 48 pph of the four different bentonites or the same quantities of bentonite, but also with 20 pph PEG 600. The data presented in (c) shows in more detail the values obtained from starch-bentonite-PEG600 mixtures. NC means the non-coated paper. The numerical values represent the average of 3 WVTR measurements and the error bars represent the standard deviation of the WVTR value for a particular coating. The absent bar represented by 'X' denotes data not obtained for this sample.

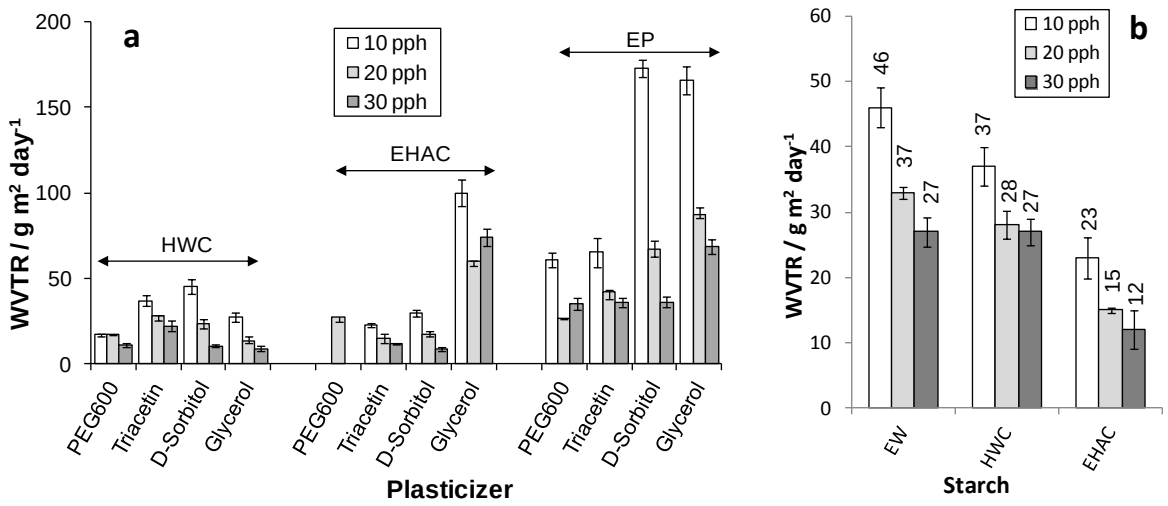

Figure 2: The effect of (a) the type and amount of plasticizer on the WVTR values when used in conjunction with CNa and the starches HWC, EHAC and EP and (b) the amount of triacetin on the WVTR values for formulations containing CNa and starches EC, HWC and EHAC. The numerical values represent the average of 3 WVTR measurements and the error bars represent the standard deviation of the WVTR value for a particular coating.

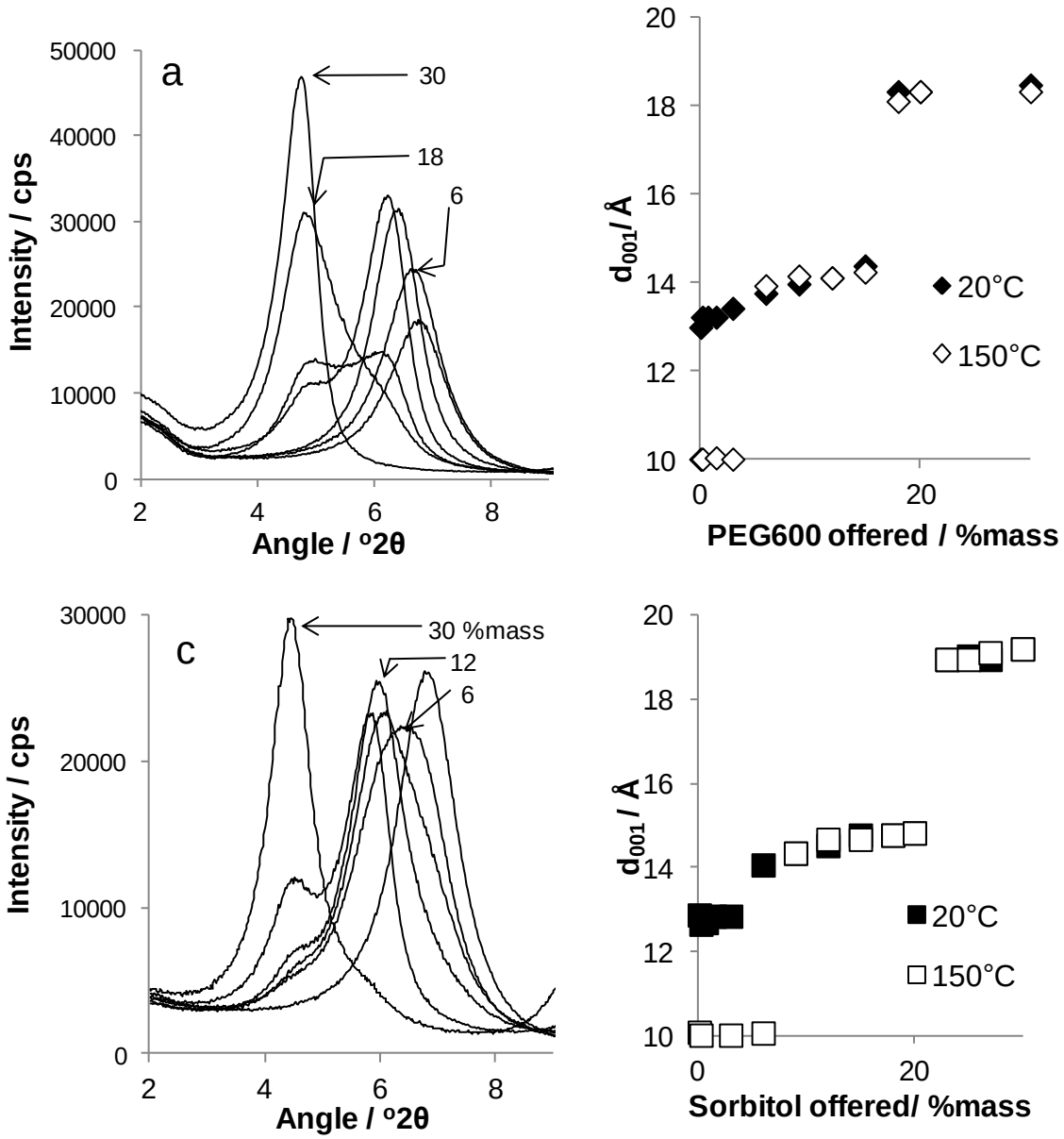

Figure 3: The effect of plasticizer loading on the X-ray diffraction traces for (a) CNa-PEG600 and (c) CNa-sorbitol together with the associated d-values at 20°C and after heating to 150°C for (b) CNa-PEG600 and (d) CNa-sorbitol. In these samples the numbers associated with selected reflections are in %mass and 30 %mass is equivalent to 42 pph.

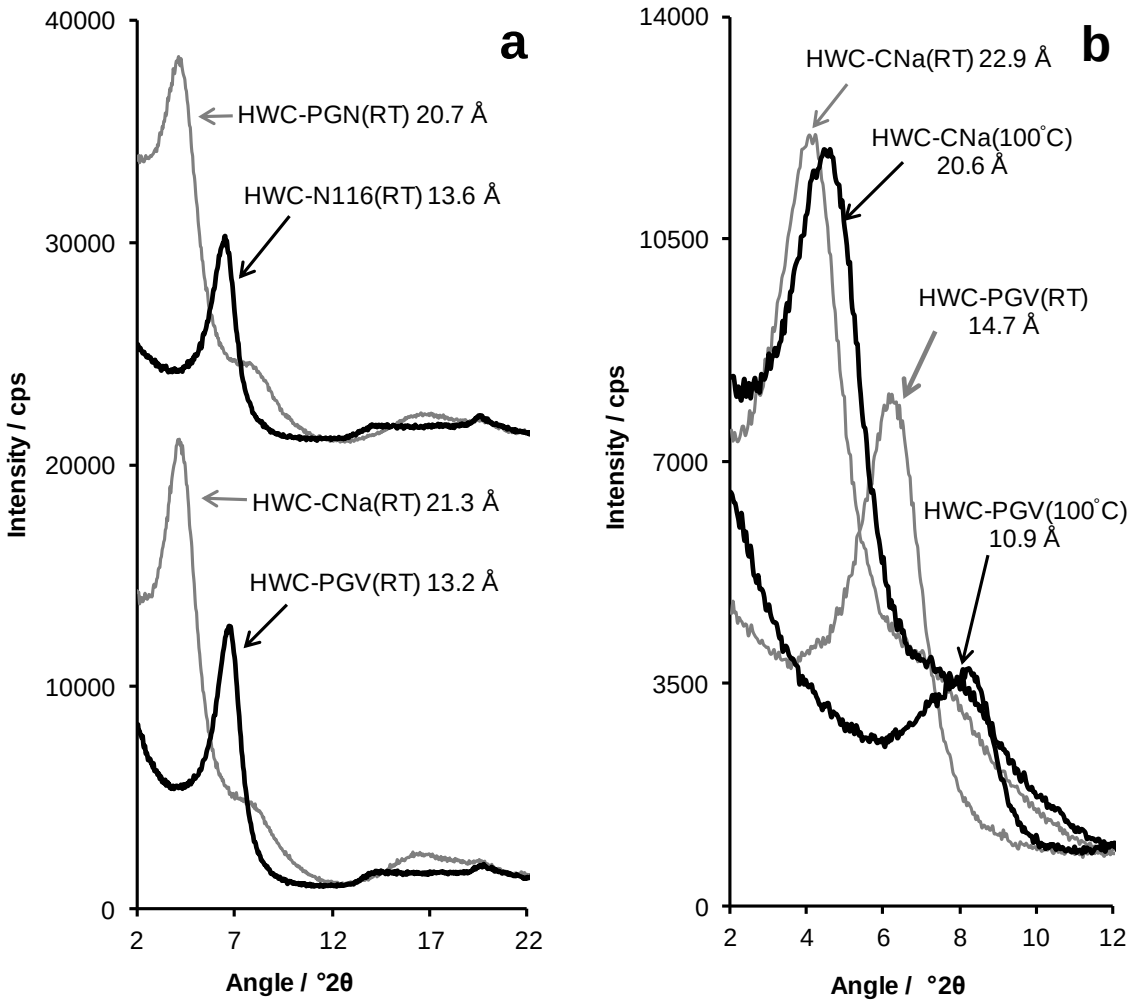

Figure 4: A comparison of the X-ray diffraction traces obtained for coatings prepared on glass slides and subsequently kept at room temperature (RT) or further dried at 100°C, (a) the bentonites PGN, N116, CNa, and PGV after mixing with starch HWC and (b) for the bentonites CNa and PGV after mixing with starch HWC and kept at room temperature or subsequent to heating at 100°C. All samples were prepared using 11.5 g starch and 5.5 g bentonite (Table 1).

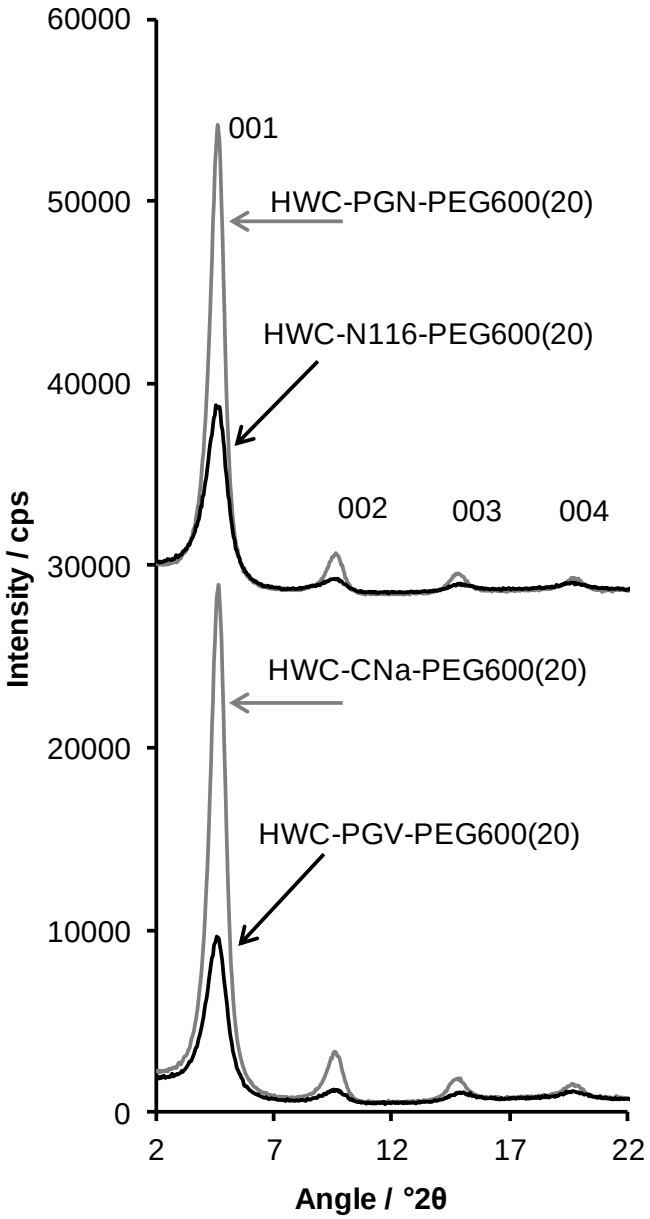

Figure 5: Comparison of X-ray diffraction profiles for the starch-bentonite-plasticizer formulations identified. Samples were prepared on glass slides.

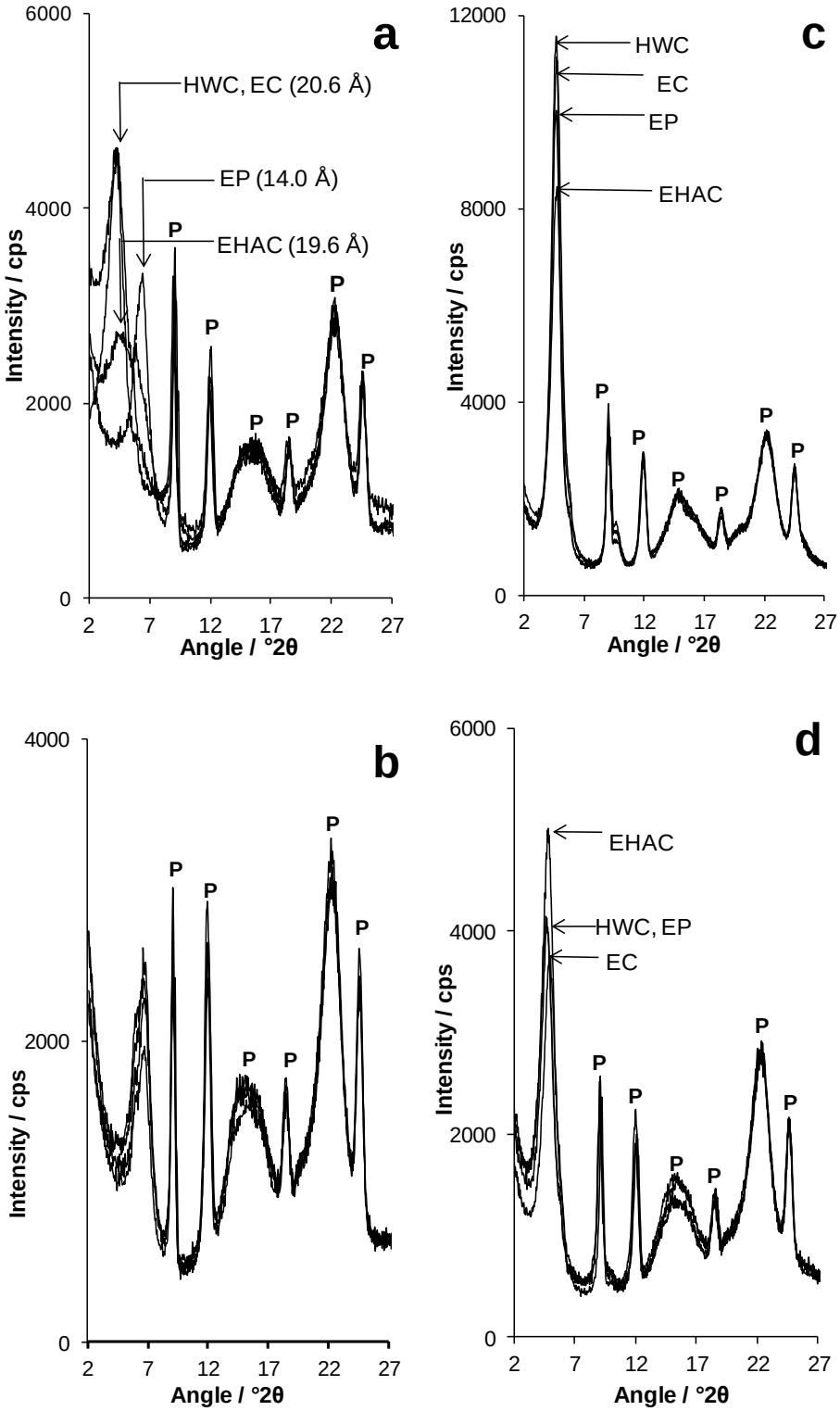

Figure 6: XRD traces obtained from paper samples coated with formulations containing (a) CNa plus starches HWC, EC, EP and EHAC, (b) PGV plus starches HWC, EC, EP and EHAC, (c) samples in (a) but with 20 pph PEG600, (d) samples in (b) but with 20 pph PEG600. P denotes a diffraction reflection from the paper substrate.

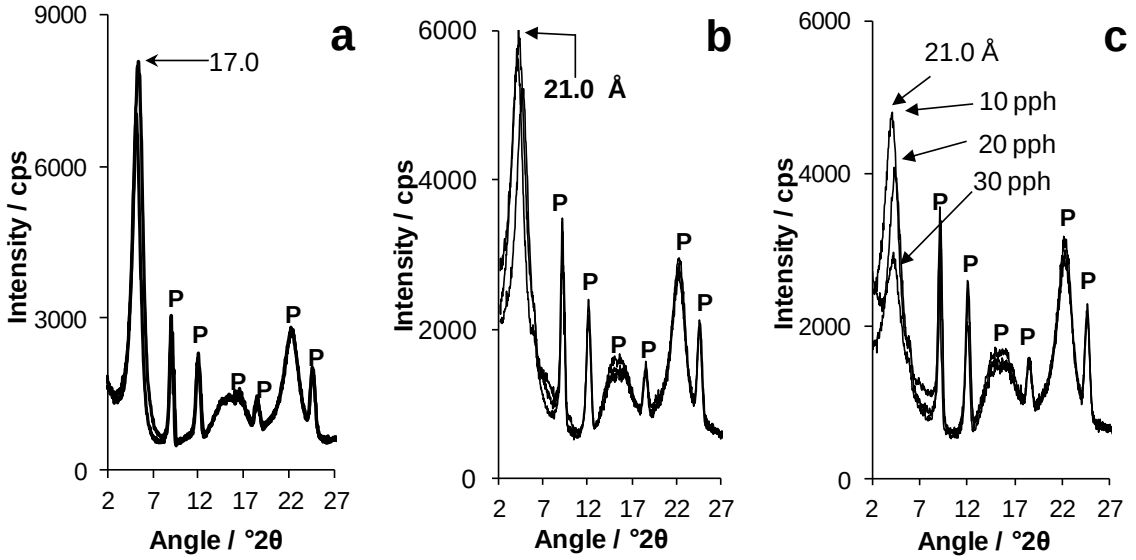

Figure 7: X-ray diffraction traces for samples of (a) CNa-HWC-triacetin (b) CNa-HWC-glycerol paper and (c) CNa-HWC-sorbitol coated on paper. Plasticizer contents were 10, 20 and 30 pph. P denotes a reflection arising from the paper substrate.

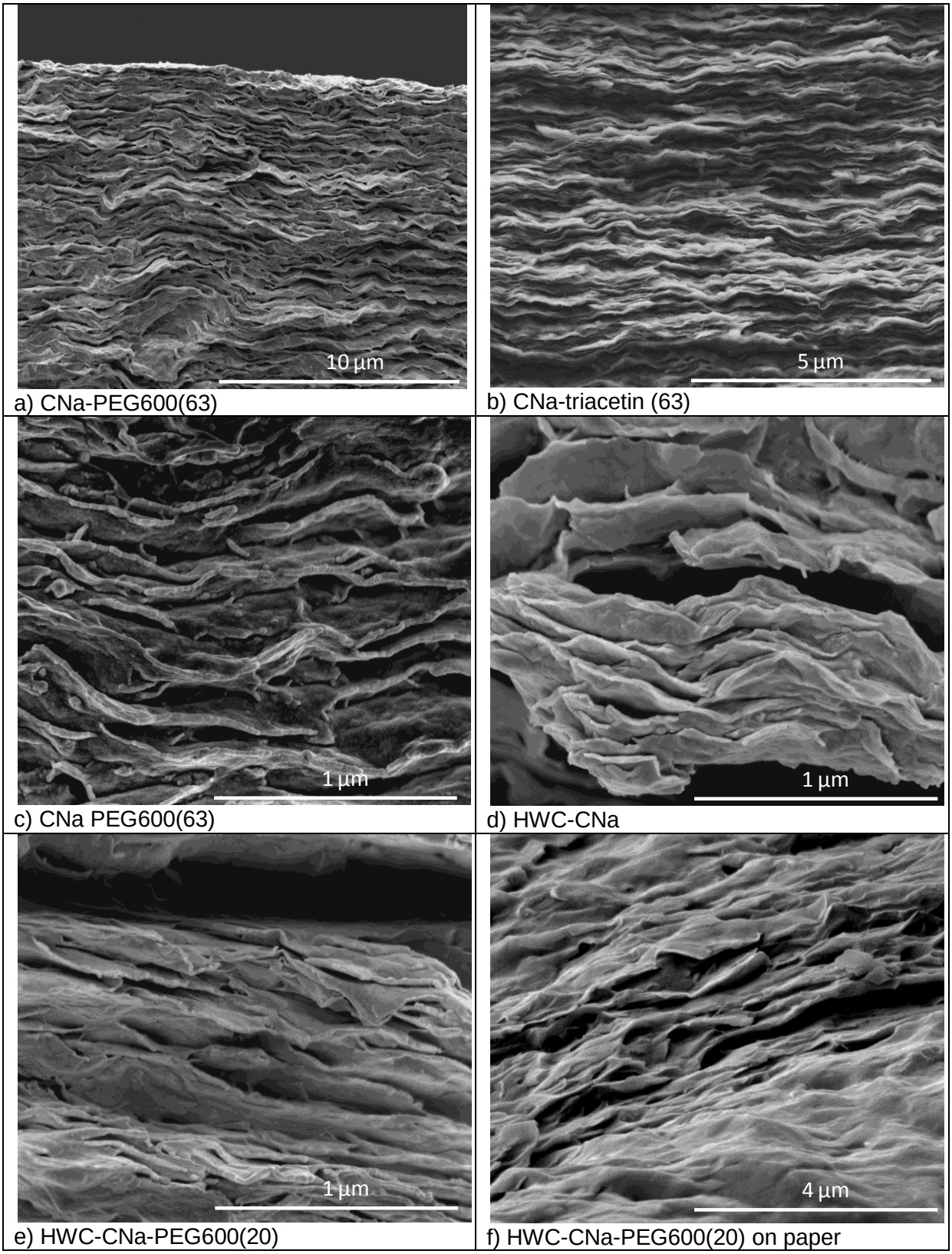

Figure 8: Scanning electron micrographs of fractured surfaces of (a) CNa-PEG600(63), (b) CNa-triacetin(63), (c) CNa PEG600(63), (d) HWC-CNa, (e) HWC-CNa-PEG600(20), and (f) HWC-CNa-PEG600(20) on paper.

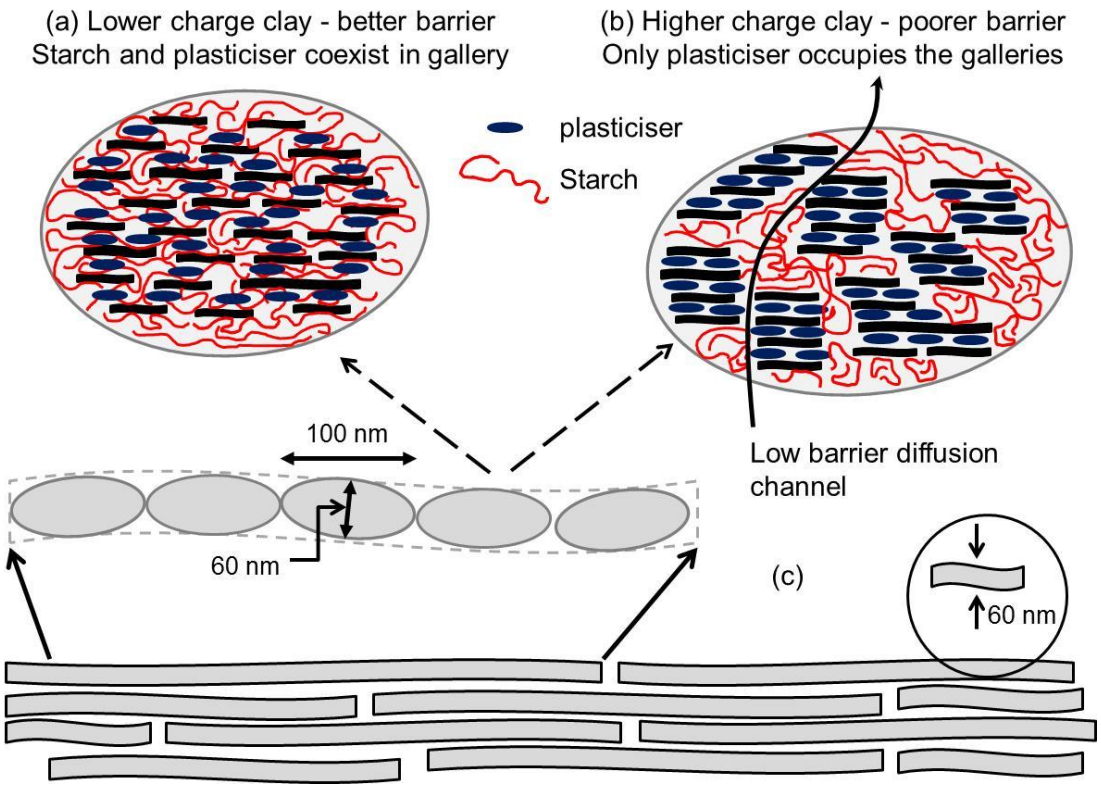

Figure 9: Schematic illustration of the different structures adopted by bentonites of lower (a) and higher (b) charge in the starch-bentonite-plasticizer globules and how they contribute to the observed 60 nm thick supramolecular layers (c).